

Effects of minor Sc addition on microstructure evolution of 2060 Al-Li alloy during homogenization

Jin Huang, Lanping Huang, Wensheng Liu

Science and Technology on High Strength Structural Materials Laboratory,

Central South University, Changsha 410083, China

E-mail address: christie@csu.edu.cn

Abstract—The microstructure evolution and composition distribution of the Sc-free and Sc-containing 2060 Al-Li alloys during homogenization have been investigated by optical microscopy (OM), scanning electron microscopy (SEM), energy dispersive spectrometry (EDS) and electron probe microanalysis (EPMA). The results indicate that serious dendritic segregation exists in the as-cast 2060 alloys. Cu element is non-uniformly distributed from grain boundaries to inside, but the variations of other alloying elements Mg, Mn and Sc are not obvious. For the Sc-free alloy, lots of coarse non-equilibrium secondary phases Al_2Cu and Al_2Cu containing Mg are continuously distributed in grain boundaries. The addition of 0.1 wt.% Sc refines the dendritic structure and non-equilibrium secondary phases in grain boundaries are mainly Al_2Cu containing Mg and Sc and $Al_6Cu(Fe)Mn$ containing Sc phases. After homogenization most of the non-equilibrium secondary phases dissolve into α (Al) matrix. For the Sc-containing alloy, the micro-segregation of Sc induces the formation of Cu-rich and Sc-containing $Al_3(Sc, Zr)$ particles in grain interiors and W (AlCuSc) phase precipitation in grain boundaries.

Keywords—Al-Li alloy; Homogenization; Microstructure; Sc addition; Segregation

I. INTRODUCTION

In recent years, the third generation Al-Li alloys have been widely utilized as the components in various fields involving aerospace, aircraft and military industries due to their outstanding physical and mechanical properties, such as low density, high strength, good formability and good fracture toughness [1-3]. These excellent performances mainly results from the addition of Li into Al matrix. For example, the addition of 1 wt.% Li make the elastic modulus

increase by 6% and the density reduce by 3%, respectively [1, 3]. Otherwise, micro-alloying is also an efficient method to improve the microstructure and enhance the properties of Al-Li alloys, such as transition element Cu, Zn, Zr and rare earth element Sc. Sc has obtained much attention because of its advantage of having both properties of rare earth elements and transition metals. It has been found that minor Sc addition significantly enhances the yield strength of Al-Mg-Li alloys due to the precipitation of the Al_3Sc phase [4]. The Al_3Sc precipitates can afford some significant effects including grain refinement, precipitation hardening and substructure strengthening [5, 6]. Cu addition into Al-Li alloys can induce Ti (Al_2CuLi) precipitation, which is the major strengthening phase in Al-Cu-Li alloys, and then obviously increase the alloy strength [7].

In Al-Cu-Li alloys, the effect of Sc on mechanical properties is closely correlated with the ratio of Cu/Li. In Al-Cu-Li alloys containing Cu content lower than 2 wt.%, minor Sc addition often improve their strength [8, 9]. However, for Al-Cu-Li alloys with high Cu content (more than 3.5 wt.%) and low Li content (less than 1.5 wt.%), minor Sc addition has led to the obvious loss of the strength [10]. It has been pointed out that the decrease of the strength is mainly ascribed to the formation of coarse W (AlCuSc) phase during homogenization [11].

2060 Al-Li alloy, one of the third generation Al-Li alloys developed by the Alcoa in 2011, have been used for aviation field. Compared with 2024-T3 and 7075-T6 alloys, the 2060-T8 alloy is used to fabricate fuselage, and upper and lower wings having 7% and 14% in weight reduction, respectively [3]. Currently, the work on the effects of Sc on the microstructure and properties of 2060 Al-Li alloy is still very little. Therefore, in this work, the influence of Sc on microstructure evolution of 2060 Al-Li alloy during

homogenization have been investigated in details.

II. EXPERIMENTAL PROCEDURES

The investigated Sc-free and Sc-containing 2060 alloys having the compositions of Al-3.8Cu-0.9Li-0.8Mg-0.35Zn-0.3Ag-0.25Mn-0.1Zr-(0.1Sc) (wt.%) were designed and prepared. To eliminate the effect of the initial cast structure, the as-cast specimens used for homogenization treatment with sizes of 10 mm×10 mm×30 mm were cut from the locations with the same diameter in the center of alloy ingots with a diameter of 103 mm and a height of 245 mm. The as-obtained specimens were homogenized at 490 °C, 500 °C and 510 °C for 24 h in salt bath furnace, respectively. The as-cast and homogenized microstructures were characterized by optical microscopy (OM), scanning electron microscopy (SEM) and electron probe microanalysis (EPMA). Grain structure was observed after being anodized with a mixed solution of 0.2 ml HF+18 ml HCl+7 ml HNO₃+42 ml H₂O and viewed with on a LEICA DM 2007 M optical microscopy. A Nava Nano 230 SEM equipped with energy dispersive X-ray spectroscopy (EDS) was used for performing the microstructural features of the alloy. Composition analysis of the selected areas and secondary particles were carried out on a EPM-800 EPMA instrument.

III. RESULTS AND DISCUSSION

Figure 1 (a) and (b) shows the OM images of the as-cast Sc-free and Sc-containing 2060 alloys. The as-cast 2060 alloys consist of dendritic or cellular dendritic α (Al) grains and lots of non-equilibrium secondary phases distributed along the grain boundaries and in the inter-dendritic regions. The high magnification SEM images and the element mappings of the as-cast 2060 Al-Li alloys detected by EPMA are presented in Fig.2. A great number of coarse non-equilibrium phases are distributed in the Sc-free alloy, as the white net-like parts shown in Fig. 2(a1), but in the Sc-containing alloy, continuous secondary phases obviously decrease and discontinuous small particles increase, as shown in Fig. 2(a2). The distribution of the alloying elements Cu, Mg and Zn are indicated in Fig. 2 (b1)-(d2). Li is hard to be detected due to its light weight. The distribution images of Ag and Zn elements are not shown here because it is difficult to distinguish their segregations due to their low contents [12].

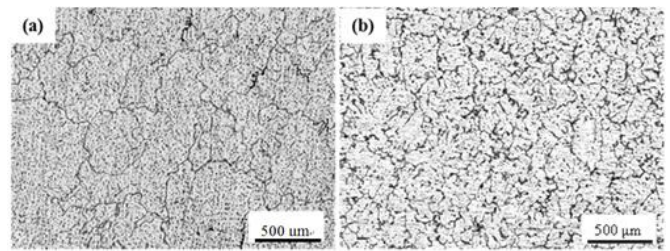


Figure 1 OM images of the as-cast Sc-free and Sc-containing 2060 alloys: (a) Sc-free 2060 alloy; (b) Sc-containing 2060 alloy

Cu is enriched in grain boundaries and dendritic regions. Mg and Mn are also found to be enriched in some areas of grain boundaries. In the dendritic regions, Cu is non-uniformly distributed, but the Cu distribution in the Sc-free alloy is more heterogeneous than that in the Sc-containing alloy. The variations of Mg and Mn are not obvious for both the alloys. To eliminate serious segregation of the alloying elements in dendritic regions, the homogenization treatment is required before thermoplastic deformation. Otherwise, as shown in Fig. 2(f), Sc is relatively uniformly distributed in the Sc-containing Alloy.

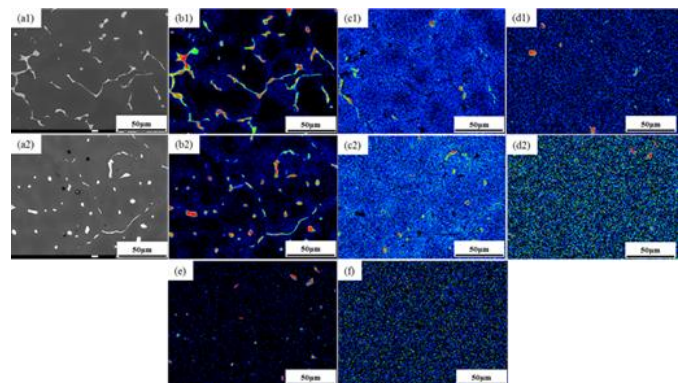


Figure 2 High magnification SEM images (a1, a2) and the element mappings of Cu (b1, b2), Mg (c1, c2), Mn (d1, d2), Fe (e) and Sc (f) in the as-cast Sc-free (a1-d1) and Sc-containing (a1-f) 2060 Al-Li alloys detected by EPMA

Figure 3 shows the high magnification SEM images of the non-equilibrium secondary phases for the Sc-free and Sc-containing 2060 alloys. The results of EDS analysis of six spots in Fig. 3 are listed in Table 1. According to EDS and EPMA quantitative analysis, these non-equilibrium secondary particles mainly consist of Al₂Cu phase and Al₂Cu phase containing trace Mg in the Sc-free alloy, and small Fe content is also detected in some secondary phases (Fig. 2(e) and Fig. 3(a)). For the Sc-containing alloy, the non-equilibrium phases in grain boundaries contain Sc and the Fe

content is higher, mainly consist of $Al_6Cu(Fe)Mn$ phase.

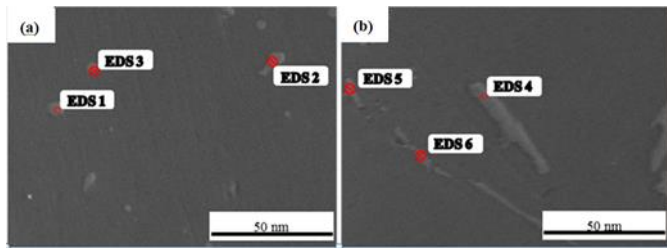


Figure 3 High magnification SEM images of the non-equilibrium secondary phases for the Sc-free and Sc-containing 2060 alloys: (a) Sc-free 2060 alloy; (b) Sc-contained 2060 alloy

Table 1 EDS analysis of as-cast 2060 alloys (at.%)

Composition ^a	Cu ^b	Mn ^c	Mg ^d	Fe ^e	Sc ^f	Al ^g
1 ^a	23.25 ^b	~ ^c	~ ^d	0.73 ^e	~ ^f	Bal ^g
2 ^a	23.91 ^b	~ ^c	~ ^d	~ ^e	~ ^f	Bal ^g
3 ^a	18.93 ^b	~ ^c	6.96 ^d	~ ^e	~ ^f	Bal ^g
4 ^a	27.52 ^b	~ ^c	2.58 ^d	~ ^e	0.89 ^f	Bal ^g
5 ^a	10.70 ^b	~ ^c	2.06 ^d	5.55 ^e	~ ^f	Bal ^g
6 ^a	21.76 ^b	2.64 ^c	~ ^d	~ ^e	0.71 ^f	Bal ^g

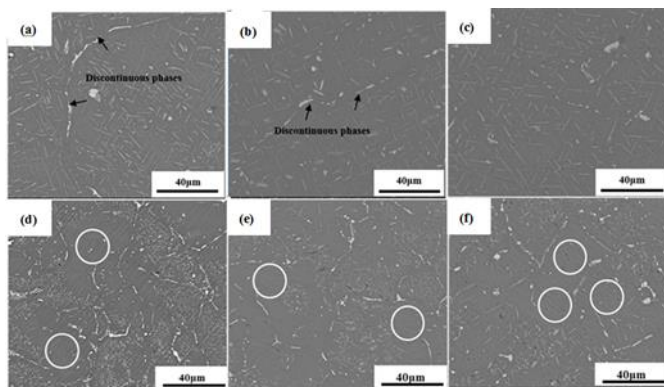


Figure 4 SEM images of the Sc-free (a-c) and Sc-containing (d-f) alloys homogenized at 490 °C (a, d), 500 °C (b, e) and 510 °C (c, f) for 24 h.

Figure 4 shows the SEM images of the Sc-free and Sc-containing alloys homogenized at various temperatures for 24 h. For the Sc-free alloy, after homogenization at 490 °C for 24 h, the dendritic structure obviously decreases and coarse secondary phases discontinuously exist in grain boundaries (Fig. 4(a)). When homogenization temperature increases to 500 °C, the dendritic structure and coarse secondary phases in grain boundaries are further reduced (Fig. 4(b)). As homogenization temperature is elevated to 510 °C, the dendritic structure and coarse secondary phases almost disappear, only fine precipitates are discontinuously distributed in grain boundaries (Fig. 4(c)). Otherwise, a great number of the needle-like precipitates exist in grain interiors

after homogenization and its amount decreases with the increase of homogenization temperature. For the Sc-containing alloy, as shown in Fig. 4(d)-(f), the dendritic structure is reduced but continuous coarse secondary phases in grain boundaries do not distinctly change after homogenized at 490 °C, 500 °C and 510 °C for 24 h. Significantly, the precipitation in grain interiors decreases for the Sc-containing alloy, even does not take place in some areas, as white circles labeled in Fig. 4(d)-(f).

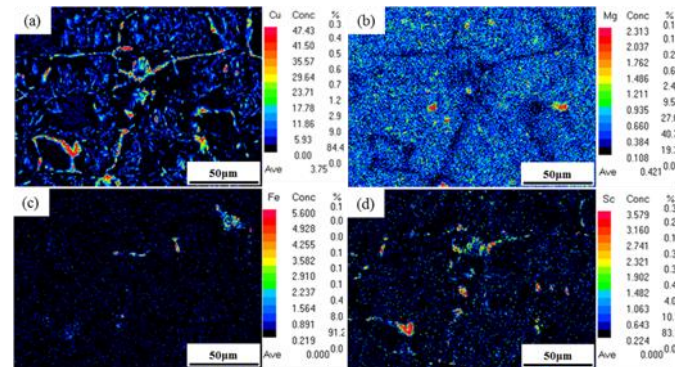


Figure 5 Element mappings of Cu, Mg, Fe and Sc for the Sc-containing 2060 Al-Li alloy homogenized at 500 °C for 24 h characterized by EPMA: (a) Cu; (b) Mg; (c) Fe; (d) Sc

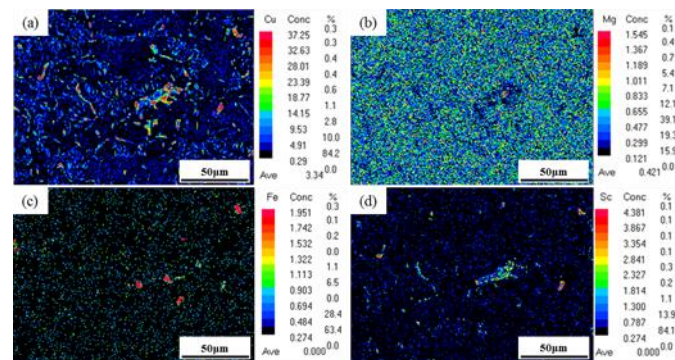


Figure 5 Element mappings of Cu, Mg, Fe and Sc for the Sc-containing 2060 Al-Li alloy homogenized at 510 °C for 24 h characterized by EPMA: (a) Cu; (b) Mg; (c) Fe; (d) Sc

Figure 5 and 6 present the element mappings of Cu, Mg, Fe and Sc for the Sc-containing 2060 Al-Li alloy homogenized at 500 °C and 510 °C for 24 h characterized by EPMA, respectively. After homogenization, Cu, Fe and Sc atoms tend to concentrate together in some particles. The element mapping of Sc in Fig. 5 (d) shows that Sc segregates in grain boundaries and forms coarse particles. Fe atoms also exhibit the similar segregation feature (Fig. 5(c)). This coarse phase

with Cu-rich and Sc is W (AlCuSc) phase. When homogenization temperature attain to 510 °C, Mg element almost dissolve into the α (Al) matrix (Fig. 6(b)), meaning that the micro-segregation of Mg is successfully eliminated by homogenization. The color of the particles containing Sc becomes slight (Fig. 6(d)). It is obvious that the Sc content decreases after increasing homogenization temperature, but Sc does not completely dissolve into the matrix and Sc segregation still exists in grain boundaries.

IV. CONCLUSION

In summary, the effects of the microstructure evolution and composition distribution of the Sc-free and Sc-containing 2060 Al-Li alloys before and after homogenization have been investigated. It is found that severe dendritic segregation and coarse non-equilibrium secondary phases continuously distributed in grain boundaries occur in the as-cast 2060 alloys. For the as-cast Sc-free alloy, secondary phases in grain boundaries are mainly Al₂Cu and Al₂Cu containing trace Mg, while the main secondary phases in grain boundaries are Al₂Cu containing Mg and Sc and Al₆Cu(Fe)Mn containing Sc phases in the as-cast Sc-containing alloy. The dendritic structure of the Sc-free 2060 alloy is reduced by minor Sc addition and Sc is uniformly distributed. Cu element is enriched in grain boundaries, but the Cu distribution in the as-cast Sc-free alloy is more heterogeneous than that in the as-cast Sc-containing alloy. The variations of Mg and Mn are not obvious. After homogenization, most of the

non-equilibrium secondary phases dissolve into α (Al) matrix. For the Sc-containing alloy, the micro-segregation of Sc induces the formation of Cu-rich and Sc-containing nanoscale Al₃(Sc, Zr) particles in grain interiors and W (AlCuSc) phase precipitation in grain boundaries.

ACKNOWLEDGMENT

The work was primarily financial supported by Science and Technology on High Strength Structural Materials Laboratory, Central South University.

REFERENCES

- [1] R. J. Rioja, J. Liu. *Metall Mater Trans A*. 2012, 43, 3325-3337.
- [2] T. Dursun, C. Soutis, *Mater. Des.* 2014, 56, 862–871.
- [3] A. Abd El-Aty, Y. Xu, X. Z. Guo, S. H. Zhang, Y. Ma, D. Y. Chen. *J Adv Res* 2018, 10, 49-67.
- [4] M. J. Birt, R. A. Halfey, J. A. Wagner. *Scripta Metall Mater.* 1993, 28(8), 919-923.
- [5] M. J. Starink, N. Gao, N. Kamp, S. C. Wang, P. D. Pitcher, I. Sinclair. *Mater Sci Eng A*. 2006, 418(1-2), 241-249.
- [6] Y. Wang, H. Y. Liu, X. C. Ma, R. Z. Wu, J. F. Sun, L. G. Hou, J. H. Zhang, Xi. L. Li, M. L. Zhang. *Mater Charact.* 2019, 154, 241-247.
- [7] E. Gumbmann, F.D. Geuser, C. Sigli, A. Deschamps. *Acta Mater.* 2017, 133 (4), 172-185.
- [8] V. Singh, K. S. Prasad, A. A. Gokhale. *Scripta Mater*, 2004, 50, 903-908.
- [9] Z. G. Chen, Z. Q. Zheng. *Scripta Mater*, 2004, 50, 1067-1071.
- [10] M. Jia, Z. Q. Zheng, X. F. Luo. *Mater Sci Forum*, 2014, 794-796, 1057-1062.
- [11] M. Jia, Z. Zheng, Z. Gong. *J. Alloy. Compd.* 2014, 614, 131-139.
- [12] Q. Liu, R. H. Zhu, J. F. Li, Y. L. Chen, X. H. Zhang, L. Zhang, Z. Q. Zheng. *Trans. Nonferrous Met. Soc. China.* 2016, 26, 607-619.